A remote assessment of ice-rich permafrost loss across a ~500m elevation gradient in the Mackenzie and Selwyn Mountains, Canada

Geoff G.L. Kershaw[1*]; William Quinton[1]; Steven Mamet[2] G. Peter Kershaw[3]

[1]*Department of Geography and Environmental Studies, Wilfrid Laurier University, Waterloo, ON, N2L 3C5, Canada*
[2]*Department of Soil Science, University of Saskatchewan, Saskatoon, SK, S7H 5A8, Canada*
[3]*Department of Earth and Atmospheric Sciences, University of Alberta, Edmonton, AB, T6G 2E3, Canada*
**kers7130@mylaurier.ca*

ABSTRACT

In the eastern Mackenzie and Selwyn Mountains, NT, Canada, five ice-rich permafrost ice-rich permafrost features have decreased in areal extent as permafrost temperatures and supra-permafrost thickness have increased since the mid-1990s. Among these features, thaw rates have been more rapid at higher elevations from the 1940s-1980s, while lower elevation features have more recently been decreasing in extent as peat block calving and subsidence accelerate. A comprehensive regional survey of ice-rich permafrost is necessary to assess whether these five fine-scale observations are representative of broader spatial and temporal changes in the area.

This paper explores the potential of remote sensing data to discern trends in permafrost extent across a ~500m elevation gradient within a 1757 km^2 study area. Our sample of 350 ice-rich permafrost features identified on 2010/2013 satellite images exhibited a decline in log area ($\log_A$) with increasing elevation, but no discernable association with shape index (SI) values. Aerial photographs from 1944 and 1974 were also used to assess temporal trends in permafrost extent for a subset of 33 features, including three of those previously reported on. There was a significant decline in $\log_A$ with time, and a complementing pattern in SI was observable among features >1400 m.a.s.l.. In the fall of 2017, field surveys will be conducted to confirm the elevation, dimensions, and site characteristics of each sampled feature. Further research concerning the driving variables of permafrost distribution and thaw rate variance should focus on parameters reflecting the local hydrology, vegetation, snow pack, and soil characteristics of each site.

KEYWORDS

Canada, alpine, permafrost, remote sensing, climate change

1. INTRODUCTION

Throughout the circumpolar, permafrost is thawing and receding poleward in response to a warming climate ((Osterkamp and Romanovsky, 1999; Beilman and Robinson, 2003; Saito *et al.*, 2007). This change is expected to accelerate in future (Saito *et al.*, 2007). Isolated permafrost (<10% of exposed ground surface) (Van Everdingen, 2005) is the most vulnerable to this climate induced thaw as its temperature rarely deviates from just below the freezing point depression

(Sannel and Kuhry, 2011) and a minimal shift in the annual energy balance of the soil can thaw what small volume of permafrost remains.

Montane systems, with their steep elevation gradients, have been experiencing more extreme changes in climate than lowland areas over the past 150 years (Mountain Research Initiative EDW Working Group, 2015). Assuming climate is the primary factor driving permafrost distribution, a change in elevation is expected to result in a more pronounced change in permafrost's distribution than a similar magnitude shift in latitude. For example, changes in ground temperature across 1 km elevation have been reported as high as 15°C, roughly comparable to a 1000 km latitudinal shift (Riseborough *et al.*, 2008). This creates a vital research opportunity, as the distribution of climate sensitive landforms and ecology will be more pronounced in montane settings, yet these areas remain relatively data poor (Hilbich *et al.*, 2008; Smith *et al.*, 2010). But montane permafrost models often rely on empirical relationships to air temperature (Riseborough *et al.*, 2008; Bonnaventure and Lewkowicz, 2013), as they are difficult to parameterize and execute due to landscape heterogeneity in soil characteristics, climatic conditions, plant community, slope and exposure. As a result, these models often have increased error and decreased transferability for their results (Riseborough *et al.*, 2008). Previous studies in the Mackenzie and Selwyn Mountains have described the conditions of ice-rich permafrost features between ~1200-1600 m.a.s.l., reporting general trends of linearly increasing permafrost temperature parallel to non-linearly decreasing feature extent. Detailed accounts of changing supra-permafrost thickness, aerial extent, and shape complexity continue to be made annually, while local air, ground, and soil temperature records are continuous from 1990s onward (Kershaw, 2003; Mamet *et al.*, 2017).

In areas where the peat layer is thick, substrate fine textured, saturated, and seasonal descent of the freezing front slow, permafrost often forms thick ice lenses, heaving the ground upward as the volume of water increases with phase change (Seppälä, 2011). This permafrost is more resistant to a warming climate as a large amount of latent heat is required to thaw the excess ice. When such ice-rich permafrost thaws, it often results in thermokarst pond depressions, which in turn accelerate thaw of the surrounding area via increased lateral heat conduction from the newly formed water bodies (Kurylyk *et al.*, 2016). As thermokarst areas expand, they eventually merge to create hydrological connections via fen networks where before elevated plateau's and isolated bogs prevailed (Quinton and Baltzer, 2013). In turn, the plant community previously perched above the water table must adapt, as many lichen, moss, shrub and tree species become replaced by aquatics in the process of paludification (Jorgenson *et al.*, 2001).

In this study, we use high resolution panchromatic satellite imagery from the Mackenzie Mountains to discern spatial trends in the variability of ice-rich permafrost feature extent and shape complexity across a ~500m range of elevation. We then apply a series of historical aerial photographs from the area to compare temporal changes in permafrost extent. Temporally, ice-rich permafrost features were expected to decline in size across the study area, while spatially, the size and complexity of features are expected to vary such that small, compact features are found at higher elevation while low elevation features are relatively large with complex perimeters. This study is exploratory and it's statistical techniques descriptive in nature. Future research is discussed, specifically what field assessments are necessary to parameterize the local ecological, hydrological, and soil characteristics moderating permafrost freeze/thaw processes.

METHODS

1.1 Study Area

The area of the Mackenzie Mountains considered in this study was most recently glaciated during the Gayna River Glaciation 22000 years B.P. (Kershaw and Kershaw, 2016). The ice-rich permafrost features we focus on established post glaciation, less than ~1182-1165 years ago, as evidenced by White River Tephra below aquatic and emergent plant peat layers deposited before ice lensing heaved the ground surface above the water table (Kershaw and Gill, 1979). These features are found in the valley bottoms and across broad perched plateau wetlands bog-fen-permafrost complexes (Kershaw and Gill, 1979) (Figure 1). Today these features have ice-rich soils (typically >20% ice content) with peat overburden (typically <5m) (Skaret, 1995), anomalous for alpine permafrost which is typically found in well drained and organic poor soils or exposed bedrocks (Zhang *et al.*, 1999).

While some assert such features follow cycles of formation and decay (Seppälä, 2011), this is not obvious in our study area where long-term monitoring efforts have observed permafrost thaw of ~1% per year over the past half century, with some features disappearing completely and no new features forming (Kershaw, 2003). This is consistent with observed permafrost loss throughout the circumpolar and is most likely the result of a larger climatic shift towards warmer conditions. Tree-ring records as proxy for temperature trends suggest a warmer climate occurred in the region during the late 18th century, and that it is again warming since the mid-20th century (Mamet and Kershaw, 2012).

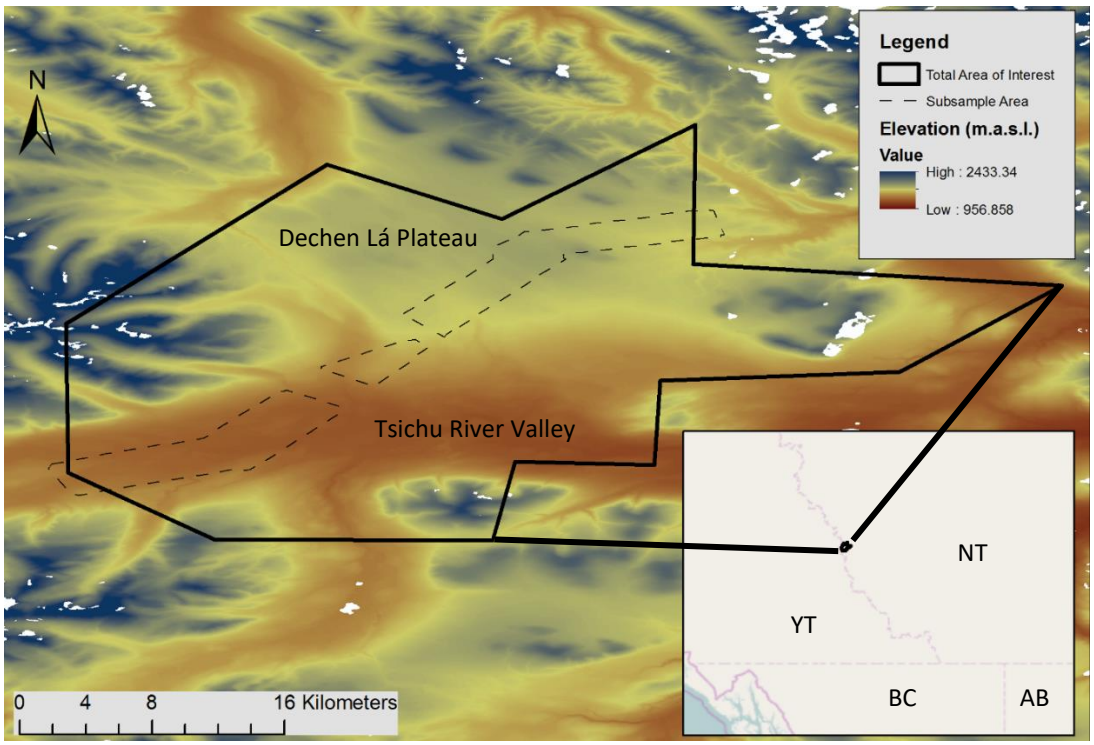

Figure 1: Map of study area. Total area of interest was limited to the maximum extent of overlapping air photos and satellite imagery, while the subsample area was limited to air photos of sufficient quality for feature delineation. The Digital Elevation Model (DEM was created by the Polar Geospatial Center from DigitalGlobe, Inc. imagery.

1.2 Data Processing

1.2.1 Image Acquisition

1944, 1948, 1949, and 1974 air photos of the study area were acquired from the National Air Photo Library (NAPL). 295 Air photos were digitized with an Epson 12000 XL scanner set at 1200 dpi. 56 air photos were georeferenced to Worldview-2 panchromatic satellite imagery from 2010/2013 (DigitalGlobe, Inc., Westminster, CO, USA). The overlapping extent of images from 2000s, 1970s, and 1940s was assigned as our total study area to survey, covering 1757 km^2. A series of 1944 and 1974 images taken at lower elevation (6000-2750 m.a.s.l.) were also selected for a 202 km^2 subsample survey as they had image quality consistent with Worldview's spatial resolution of 0.5m.

All spatial inputs were processed with ArcMap 10.3.1 GIS (ESRI, Inc., Redlands, CA, USA) projected in the datum WGS_1984. Resampling with the nearest neighbor method was done to generate digital pixel values from the scanned air photos, allowing us to georeference them to the 2010/2013 Worldview base map. Spatial distortion and scaling of each photo was corrected with 5 ground control points and an affine 1st order polynomial transformation. The Root Mean Square Errors (RMSE) resulting from this rectification were calculated to assess the accuracy of georeferencing.

1.2.2 Feature Identification

Ice-rich permafrost features were identified by their morphological traits of increased relief and distinct reflectance due to differing surface vegetation. While categorical distinctions have been made among the ice-rich permafrost features we are considering, namely palsas, peat plateaus, and pingos, this distinction cannot be made reliably with remote sensing means.

Our sample included 350 Polygons defining the perimeter of ice-rich features visible on 2010/2013 satellite images. Each feature was assigned a mean elevation as calculated with the Zonal Statistic tool in ArcGIS, linked to a Digital Elevation Model (DEM) generated by the Polar Geospatial Center from DigitalGlobe, Inc. imagery. A subsample of 33 features from across the elevation gradient had additional polygons delineating feature extent in 1944 and 1974 air photos. This subsample included three features with ongoing microclimate and active layer monitoring across the elevation gradient (Mamet *et al.*, 2017).

1.3 Data Analysis

The feature attributes considered in our analysis were log aerial extent ($\log_A$) and shape index (SI). The skew and kurtosis for area lead us to apply a log transformation to better establish normality. A Shapiro-Wilk test was run to confirm the effectiveness of the transformation. Spatial autocorrelation of feature location and areal extent values were assessed with Moran's I coefficients using the global Moran's I tool in ArcMap. SI relates the complexity of the perimeter relative to the area of the feature with the following calculation:

$$SI = 0.25 \times \frac{P}{\sqrt{A}},$$

where P is perimeter (m), and A is area (m^2). A SI value of 1 relates a maximally compact square and values >1 reflect increasing complexity (McGarigal *et al.*, 2012). Spatial and temporal trends in $\log_A$, and SI were assessed across the elevation gradient and from 1944-2013 using simple

linear regression. Temporal trends were limited to the subsample of 33 features while spatial trends considered all 350 features identified in 2010/2013 satellite imagery.

2. RESULTS AND DISCUSSION

2.1 Spatial Trends

A histogram of area values exhibited negative exponential form ($y = -6.196\ln(x) + 26.071$, $R^2 = 0.7211$). This was corrected with log transformation to assure normality and homogeneity of variance, as confirmed with a Shapiro-Wilk test (α 0.05) (data not shown). The elevation values were skewed negatively (-0.277), relating a greater concentration of features on the higher Dechen Lá plateau than the lower Tsichu valley or intervening slope (Figure 1). For $\log_A$ and elevation values, specific features were identified as potential outliers (>3x Interquartile range). After reassessing the location and extent of these features, each was found to be accurate and remained included in the sample data.

The Moran's index reported for the sample of 350 features was 0.090 with a z-score of 3.7 (p-value <0.01). Given this value, the null hypothesis was rejected and features considered spatially autocorrelated. This could result from internal or external mechanisms acting on the population. Internally, as larger coalesced fields thaw, they form groups of smaller detached features which are highly spatially autocorrelated. Externally, the conditions for formation and persistence of ice-rich permafrost could be limited to specific areas on the landscape where the slope, snow pack thickness, and substrate consisting of thick organic overburden with highly saturated fine grained clay below are conducive to ice lens formation (Seppälä, 2011).

The combination of Worldview images (0.5m resolution) and Polar Geospatial Centre DEM (5.0 m resolution) allowed for an assessment of spatial trends in $\log_A$ and SI across a ~500m elevation gradient. Log_A reported a significant negative association with elevation ($F(1,350)=11.695$, $p<0.01$). This is consistent with the initial observations of Mamet *et al.* (2017), though SI did not report a significant association with elevation, as expected ($F(1,350)=0.109$, $p=0.745$) (Figure 3).

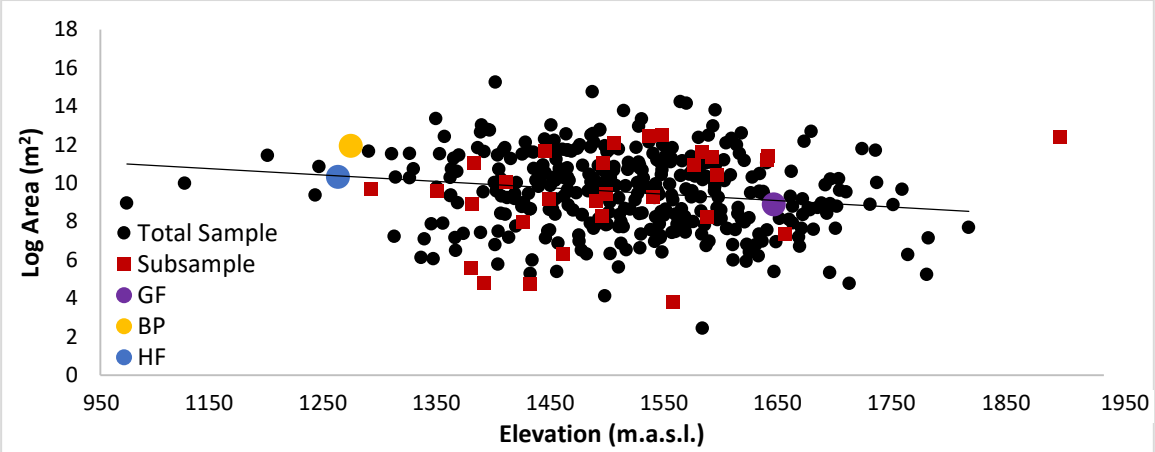

Figure 2: Elevation vs $\log_A$ in 2010/2013 for the total sample population (n=350) with a linear regression trend line of $y = -0.0839x + 24.492$ ($R^2 = 0.0324$). Subsample features and features previously assessed identified.

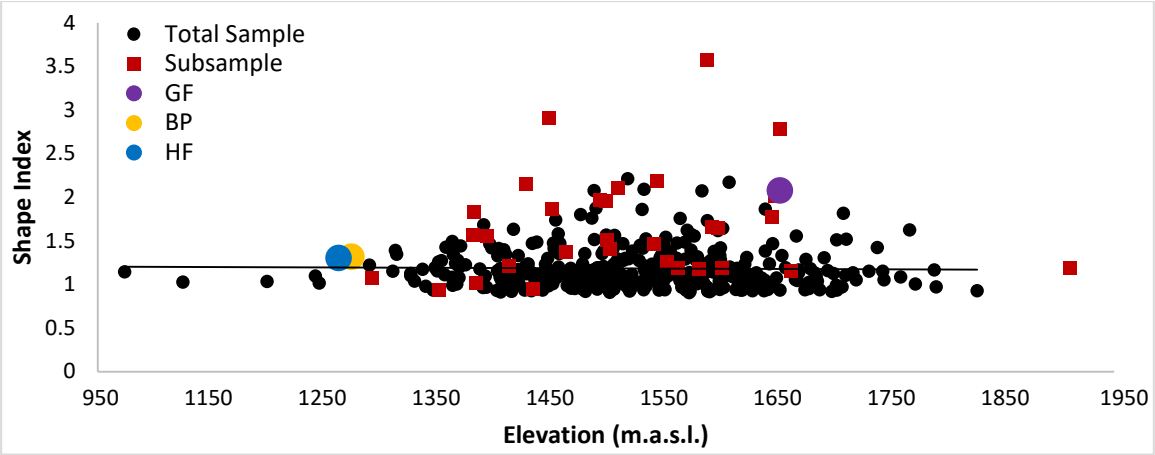

Figure 3: Elevation Vs Shape Index (SI) in 2010/2013 for the total sample population (n=350) with a linear regression trend line of y = -0.0012x + 1.3478 (R^2 = 0.0005). Subsample features and features previously assessed identified.

2.2 Temporal trends

Given the limited image quality of many of the historical air photos, we were unable to directly assess temporal trends in ice-rich feature geometry across the entire study area. Instead, we chose a subsample of features from within a reduced survey area where air photos were taken at lower elevation, providing better image quality sufficient for feature delineation (Figure 1). The features selected within this area were spaced widely in order to correct for the spatial autocorrelation reported by the larger sample. The subsample also deliberately included three features with previous monitoring of microclimate and active layer thickness for comparison with this larger sample. This technique is problematic due to the non-random nature of the subsample, but we considered it reasonable for the purposes of data exploration in this paper. The resulting Moran's index for the subsample was -0.045 with a z-score of -0.17 (p-value 0.8609) allowing us to assume spatial independence.

Previous research suggested a temporal shift towards less permafrost in our study area, with thaw more rapid at higher elevations in the 1940s-1980s while lower elevation features more rapidly decreased in extent from the 1980s onwards (Mamet *et al.*, 2017). This is consistent with our subsample data as there was a significant decline in $\log_A$ through time ($F(1,108)=22.0433$, $p<0.01$), following the regression y = -0.0161x + 43.136 (R^2=0.0916). When separating the subsample into high and low elevation features, regressions remained significant ($F(1,108)=16.7175$, $p<0.01$ and $F(1,108)=2.8225$, $p=0.03$ respectively) with a greater rate of aerial loss for high elevation features (Figure 4). We were unable to discern different rates of thaw between the two time periods of 1944-74 and 1974-2010 though, likely due to the limited sample size of the data.

Previous research also identified a temporal shift in shape complexity of ice-rich permafrost features, such that low elevation features were increasing in complexity from the 1980s onwards while high elevation features have transitioned through this period before the 1980s and are more recently reducing in complexity (Mamet *et al.*, 2017). In this study, there was no significant linear trend to the subsample's change in SI ($F(1,108)=3.3308$, $p=0.07$), but when low and high elevation features were considered separately, features >1400 m.a.s.l. reported a significant increase in SI through time ($F(1,59)=16.7175$, $p=0.01$) (Figure 5). This discrepancy is interesting,

but may in part be due to limited sample size as only 10 features were identified <1400 m.a.s.l. compared to the 20 at >1400 m.a.s.l.. It is also important to consider that the observed changes may only be a small portion of the trajectory of permafrost thaw for these features. The maximum extent of these ice-rich permafrost features most likely was much reduced before our period of assessment. In Alaska for example, tree ring and carbon isotope analysis has been generated an estimate that 83% of permafrost's maximum extent had been lost before 1949 (Jorgenson *et al.*, 2001). This would affect the SI values we could expect to observe as the features are likely small and simple relative to their previous maximum extent.

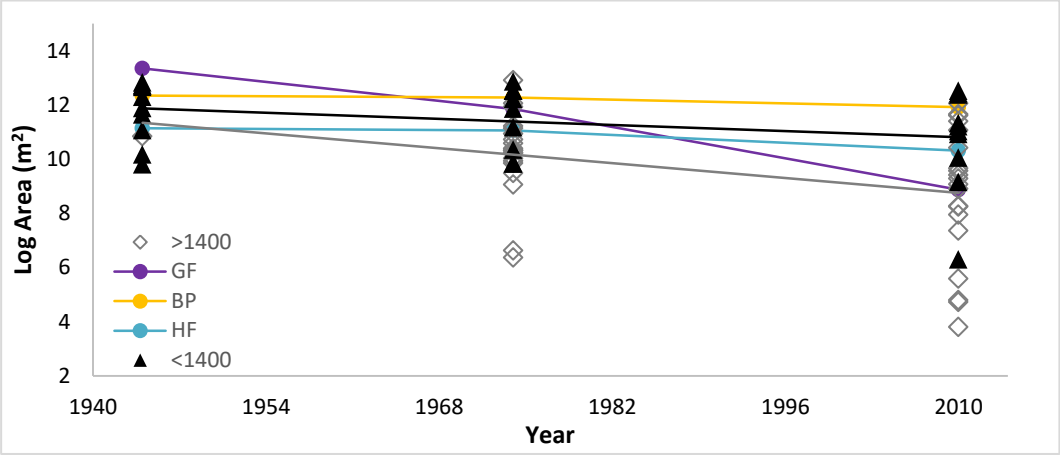

Figure 4: Log area Vs time for the subsample of ice-rich permafrost features (n=33). Goose Flats (GF) at 1625 m.a.s.l., Beaver Pond (BP) at 1275 m.a.s.l., Hare Foot (HF) at 1260 m.a.s.l. identified, as well as features >1400 m.a.s.l. ($y = -0.0357x – 80.581$ ($R^2 = 0.2237$)) and features <1400 m.a.s.l. ($y = -0.0161x + 43.136$ ($R^2 = 0.0916$))

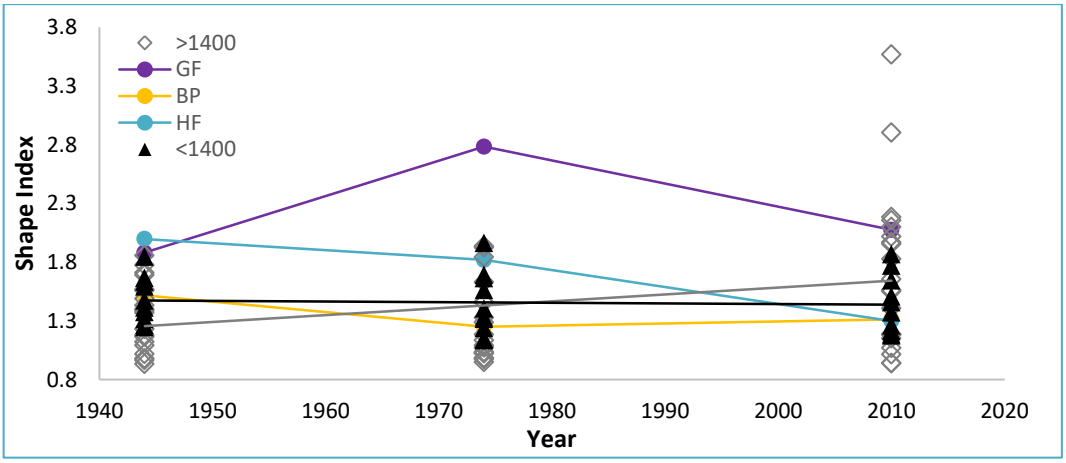

Figure 5: Shape index Vs time for the subsample of ice-rich permafrost features (n=33). Goose Flats (GF) at 1625 m.a.s.l., Beaver Pond (BP) at 1275 m.a.s.l., Hare Foot (HF) at 1260 m.a.s.l. identified, as well as features >1400 m.a.s.l. ($y = 0.0058x - 10.19$ ($R^2 = 0.1013$)) and features <1400 m.a.s.l. ($y = -0.0005x + 2.5171$ ($R^2 = 0.004$))

2.3 Future Research

As this paper is exploratory and descriptive in nature, there is a series of analytical options for expanding the study design. Statistically, spatial autocorrelation was an issue with our total sample. While this was corrected with a selective subsample maximizing coverage and minimizing autocorrelation, data transformations like the generalized least squares and conditional autoregressive models may be more effective at this task as they do not compromise randomness of sample selection (F. Dormann *et al.*, 2007). Also, the process of feature identification could be expanded to include proximity to open water, slope, estimated elevation temperature lapse rates, and other attributes that can be defined by remote means.

The use of trained categorization techniques based on pixel brightness values could also help reduce error in feature delineation, depending on how effectively the program could be trained and automated. Field verification could then follow to confirm the presence/absence of permafrost and open water where shadowing and aquatic vegetation obscure feature edges. Such a ground-truthing campaign would require a more recent set of satellite images as the features in question may have changed in the four years since worldview last produced images of the area.

Field verification would also be an opportunity to distinguish palsa, peat plateau, and pingo feature types, as well as parameterize components of mass-energy coupled equations applied in models of permafrost thaw. This parameterization would include soil characteristics such as thermal conductivity, porosity, ice and moisture content, as well as vegetation characteristics such as surface roughness and albedo.

3. CONCLUSIONS

In the valley bottoms and shallow sloped plateaus of the Mackenzie Mountains, ice-rich permafrost features form in wetlands under thick insulating layers of peat, thin snow pack, and where subsurface water is readily available for ice lens formation. This project provides an exploratory assessment of the potential remote sensing data has for quantifying changes in the distribution of ice-rich permafrost features in montane environments. The acquisition, processing, and analysis of historical air photo and satellite images from 1944-2013 is described and the limits of such an approach discussed - namely issues of historical image quality, spatial autocorrelation, and sample size. We describe spatial and temporal patterns in the distribution of ice-rich permafrost across a ~500m elevation gradient. Spatially, Log_A decreases with elevation. Temporally, Log_A has been in decline since 1944. The general trend of declining extent is consistent with previous observations across the elevation gradient. Temporally, SI was unresponsive to changes in elevation and time, unless features >1400 m.a.s.l. were considered alone, whereby an increase in SI through time was observed. A larger sample of features across the elevation gradient, particularly at lower elevations, would likely increase confidence in the observed temporal trends. The discrepancy between changes in low and high elevation Log_A and SI raises the question of what factor(s) are responsible for the distinct trends in thaw rate and shape complexity. Future research should focus on field verification and parameterization of the factors considered in soil freeze/thaw models, providing the data necessary for inferential statistical tests based on explanatory variables of microclimate, soil, hydrology, and vegetation.

ACKNOWLEDGEMENTS

This project has been supported financially by the Natural Sciences and Engineering Research Council of Canada, the Northern Scientific Training Program, and Earthwatch International (EI). We are grateful to all the EI volunteers who have joined our research team in the field over the years, as well as all the staff from Dechen Lá lodge, particularly Norm, Barb, and Josh Barichello. The DEMs used in our spatial analysis were provided by the Polar Geospatial Center under NSF OPP awards 1043681, 1559691 and 1542736.

REFERENCES

Beilman, D. & Robinson, S. 2003 Peatland permafrost thaw and landform type along a climatic gradient. *Proceedings of the 8th International Conference on Permafrost* 1, 61–65.

Bonnaventure, P.P. & Lewkowicz, AG. 2013 Impacts of mean annual air temperature change on a regional permafrost probability model for the southern Yukon and northern British Columbia, Canada. *Cryosphere* 7(3), 935–946. DOI: 10.5194/tc-7-935-2013

Bowden, W.B., Gooseff, M.N., Balser, A., Green, A., Peterson, B.J. & Bradford, J. 2008 Sediment and nutrient delivery from thermokarst features in the foothills of the North Slope , Alaska : Potential impacts on headwater stream ecosystems. *Journal of Geophysical Research* 113, 1–12. DOI: 10.1029/2007JG000470

Van Everdingen, R. 2005 Multi-language glossary of permafrost and related ground-ice terms. *National Snow and Ice Data Center/World Data Center for Glaciology, Boulder* 1998 (ed 1998 revised). DOI: 10.2307/1551636

Dormann, F., McPherson, M., Araújo, B., Bivand, R., Bolliger, J., Carl, G., Davies, G., Hirzel, A., Jetz, W. & Kissling, W. 2007 Methods to account for spatial autocorrelation in the analysis of species distributional data: A review. *Ecography* 30(5), 609–628.

Harris, I., Jones, P.D., Osborn, T.J. & Lister, D.H. 2014 Updated high-resolution grids of monthly climatic observations - the CRU TS3.10 Dataset. *International Journal of Climatology* 34(3), 623–642. DOI: 10.1002/joc.3711

Hayashi, M. 2013 The Cold Vadose Zone: Hydrological and Ecological Significance of Frozen-Soil Processes. *Vadose Zone Journal* 12, 2136. DOI: 10.2136/vzj2013.03.0064

Hilbich, C., Hauck, C., Hoelzle, M., Scherler, M., Schudel, L., Völksch, I., Vonder Mühll, D. & Mäusbacher, R. 2008 Monitoring mountain permafrost evolution using electrical resistivity tomography: A 7-year study of seasonal, annual, and long-term variations at Schilthorn, Swiss Alps. *Journal of Geophysical Research: Earth Surface* 113(1), 1–12.

Jorgenson, M.T., Racine, C.H., Walters, J.C. & Osterkamp, T.E. 2001 Permafrost degradation and ecological changes associated with a warming climate in central Alaska. *Climatic Change* 48(4), 551–579. DOI: 10.1023/A:1005667424292

Kershaw, G.P. 2003 Permafrost landform degradation over more than half a century Macmillan/Caribou Pass region, NWT/Yukon, Canada. *Permafrost, Proceedings of the Eighth International Conference on Permafrost, Ziirich, July 21-25th, pp. 543-548*

Kershaw, G.P. & Gill, D. 1979 Growth and decay of palsas and peat plateaus in the Macmillan Pass - Tsichu River area, Northwest Territories, Canada. *Canadian Journal of Earth Sciences* 16, 1362–1374.

Kershaw, G.P. & Kershaw, J.L. 2016 *A Guide To The Canol Heritage Trail and Doı T'oh Territorial Park Reserves. Norman Wells Historical Society: Norman Wells, NT.*

Kurylyk, B.L., Hayashi, M., Quinton, W.L., McKenzie, J.M. & Voss, C.I. 2016 Influence of

vertical and lateral heat transfer on permafrost thaw, peatland landscape transition, and groundwater flow. *Water Resources Research* 52(2),1286–1305.

Mamet, S.D. & Kershaw, G.P. 2012 Subarctic and alpine tree line dynamics during the last 400 years in north-western and central Canada. *Journal of Biogeography* 39(5), 855–868. DOI: 10.1111/j.1365-2699.2011.02642.x

Mamet, S.D., Chun, K.P., Kershaw, G.G.L., Loranty, M.M. & Kershaw, G.P. 2017 Recent Increases in Permafrost Thaw Rates and Areal Loss of Palsas in the Western Northwest Territories, Canada. *Permafrost and Periglacial Processes* (March) DOI: 10.1002/ppp.1951

McGarigal, K., Cushman, S. & Ene, E. 2012 FRAGSTATS V4 Available at: http://www.umass.edu/ landeco/research/fragstats/fragstats.html

Morris, A.J., Donovan, J.J. & Strager, M. 2009 Geospatial analysis of climatic and geomorphic interactions influencing stream discharge, Appalachian Mountains, USA. *Environmental Modeling and Assessment* 14(1), 73–84. DOI: 10.1007/s10666-008-9145-7

Mountain Research Initiative EDW Working Group. 2015 Elevation-dependent warming in mountain regions of the world. *Nature Climate Change* 5(5), 424–430. DOI: 10.1038/nclimate2563\rhttp://www.nature.com/nclimate/journal/v5/n5/abs/nclimate2563.html#supplementary-information

Osterkamp, T.E. & Romanovsky, V.E. 1999 Evidence for warming and thawing of discontinuous permafrost in Alaska. *Permafrost and Periglacial Processes* 10(1), 17–37. DOI: 10.1002/(SICI)1099-1530(199901/03)10:1<17::AID-PPP303>3.0.CO;2-4

Quinton, W.L. & Baltzer, J.L. 2013 Changing surface water systems in the discontinuous permafrost zone : implications for streamflow. *H02, IAHS-IAPSO-ASPEI Assembly, Gothenburg, Sweden*, July 22-26, pp. 85–92.

Riseborough, D., Shiklomanov, N., Etzelmu, B., Gruber, S. & Marchenko, S. 2008 Recent Advances in Permafrost Modelling. *Permafrost and Periglacial Processes* 156, 137–156. DOI: 10.1002/ppp

Saito, K., Kimoto, M., Zhang, T., Takata, K. & Emori, S. 2007 Evaluating a high-resolution climate model : Simulated hydrothermal regimes in frozen ground regions and their change under the global warming scenario. 112, 1–19. DOI: 10.1029/2006JF000577

Sannel, A.K. & Kuhry, P. 2011 Warming-induced destabilization of peat plateau/thermokarst lake complexes. *Journal of Geophysical Research: Biogeosciences* 116(3), 1-16. DOI: 10.1029/2010JG001635

Seppälä, M. 2011 Synthesis of studies of palsa formation underlining the importance of local environmental and physical characteristics. *Quaternary Research* 75(2), 366–370. DOI: 10.1016/j.yqres.2010.09.007

Skaret, K. 1995 *Stratigraphic, microclimatic and thawing attributes associated with palsas located in the alpine tundra environment of the MacMillan Pass - Tsichu River region, N.W.T., Canada*. Department of Geography, University of Alberta, Canada, unpublished.

Smith, S.L., Romanovsky, V.E., Lewkowicz, A.G., Burn, C.R., Allard, M., Clow, G.D., Yoshikawa, K. & Throop, J. 2010 Thermal State of Permafrost in North America : A Contribution to the International Polar Year. *Permafrost and Periglacial Processes* 21, 117–135. DOI: 10.1002/ppp.690

Zhang, T., Barry, R.G., Knowles, K., Heginbottom, J.A. & Brown, J. 1999 Statistics and characteristics of permafrost and ground-ice distribution in the Northern Hemisphere. *Polar Geography* 23(2), 132–154. DOI: 10.1080/10889370802175895